ASN NEURO RESEARCH ARTICLE

supplementary data

ASN NEURO 4(1):art:e00075.doi:10.1042/AN20110059

# Plasmalemmal $Na^+/Ca^{2+}$ exchanger modulates $Ca^{2+}$-dependent exocytotic release of glutamate from rat cortical astrocytes

**Reno C Reyes*,†, Alexei Verkhratsky‡,§ and Vladimir Parpura*,§,¶1**

*Department of Neurobiology, Center for Glial Biology in Medicine, Atomic Force Microscopy and Nanotechnology Laboratories, Civitan International Research Center, Evelyn F. McKnight Brain Institute, University of Alabama, Birmingham, AL 35294, U.S.A.

†Department of Neurology, University of California, San Francisco and Veterans Affairs Medical Center, San Francisco, CA 94121, U.S.A.

‡Faculty of Life Sciences, The University of Manchester, Manchester, M13 9PT, U.K.

§IKERBASQUE, Basque Foundation for Science, 48011, Bilbao, Spain

¶School of Medicine, University of Split, 21000 Split, Croatia

**Cite this article as:** Reyes RC, Verkhratsky A and Parpura V (2012) Plasmalemmal $Na^+/Ca^{2+}$ exchanger modulates $Ca^{2+}$-dependent exocytotic release of glutamate from rat cortical astrocytes. ASN NEURO 4(1):art:e00075.doi:10.1042/AN20110059

## ABSTRACT

Astroglial excitability operates through increases in $Ca^{2+}_{cyt}$ (cytosolic $Ca^{2+}$), which can lead to glutamatergic gliotransmission. In parallel fluctuations in astrocytic $Na^+_{cyt}$ (cytosolic $Na^+$) control metabolic neuronal-glial signalling, most notably through stimulation of lactate production, which on release from astrocytes can be taken up and utilized by nearby neurons, a process referred to as lactate shuttle. Both gliotransmission and lactate shuttle play a role in modulation of synaptic transmission and plasticity. Consequently, we studied the role of the PMCA (plasma membrane $Ca^{2+}$-ATPase), NCX (plasma membrane $Na^+/Ca^{2+}$ exchanger) and NKA ($Na^+/K^+$-ATPase) in complex and coordinated regulation of $Ca^{2+}_{cyt}$ and $Na^+_{cyt}$ in astrocytes at rest and upon mechanical stimulation. Our data support the notion that NKA and PMCA are the major $Na^+$ and $Ca^{2+}$ extruders in resting astrocytes. Surprisingly, the blockade of NKA or PMCA appeared less important during times of $Ca^{2+}$ and $Na^+$ cytosolic loads caused by mechanical stimulation. Unexpectedly, NCX in reverse mode appeared as a major contributor to overall $Ca^{2+}$ and $Na^+$ homoeostasis in astrocytes both at rest and when these glial cells were mechanically stimulated. In addition, NCX facilitated mechanically induced $Ca^{2+}$-dependent exocytotic release of glutamate from astrocytes. These findings help better understanding of astrocyte-neuron bidirectional signalling at the tripartite synapse and/or microvasculature. We propose that NCX operating in reverse mode could be involved in fast and spatially localized $Ca^{2+}$-dependent gliotransmission, that would operate in parallel to a slower and more widely distributed gliotransmission pathway that requires metabotropically controlled $Ca^{2+}$ release from the ER (endoplasmic reticulum).

Key words: astrocyte, calcium, calcium signalling, glutamate release, sodium, sodium-calcium exchanger.

## INTRODUCTION

Multiple pathways are utilized for bi-directional astrocyte-neuron signalling in various regions of the CNS (central nervous system) particularly at the synaptic level (Araque et al., 1999a; Haydon and Carmignoto, 2006; Ni et al., 2007; Theodosis et al., 2008; Perea and Araque, 2009). It is at these locations that astrocytes by using their ionotropic and metabotropic receptors listen to neurotransmission. Here, activation of astrocytic receptors leads to dynamic changes in $Ca^{2+}_{cyt}$ and $Na^+_{cyt}$ (cytosolic $Ca^{2+}$and cytosolic $Na^+$) (Lalo et al., 2011). It is also at the tripartite synapse that astrocytes, via

[1] To whom correspondence should be addressed (email vlad@uab.edu).

**Abbreviations:** AMPA, α-amino-3-hydroxy-5-methylisoxazole-4-propionic acid; BAPTA-AM, 1,2-bis-(o-aminophenoxy)ethane-*N,N,N′,N′*-tetra-acetic acid tetrakis-acetoxymethyl ester; $Ca^{2+}_{cyt}$, cytosolic $Ca^{2+}$; $[Ca^{2+}]_{cyt}$, $Ca^{2+}_{cyt}$, concentration; CNS, central nervous system; ECS, extracellular space; ER, endoplasmic reticulum; GDH, glutamate dehydrogenase; $InsP_3$, inositol 1,4,5-trisphosphate; KB-R7943, 2-[2-[4-(4- nitrobenzyloxy)phenyl]ethyl]isothiourea methane sulfonate; LSD, least significant difference; mGluR, metabotropic glutamate receptor; $Na^+_{cyt}$, cytosolic $Na^+$; $[Na^+]_{cyt}$, $Na^+_{cyt}$, concentration; NCX, $Na^+/Ca^{2+}$ exchanger; NCKX, $K^+$-dependent NCX; NKA $Na^+/K^+$-ATPase; PEI, polyethyleneimine; PMCA, plasma membrane $Ca^{2+}$-ATPase; SERCA, sarcoplasmic/endoplasmic reticulum $Ca^{2+}$-ATPase; TRPC, canonical transient receptor potential.

their $Na^+$-dependent metabolic changes (Magistretti, 2006) and by utilizing their $Ca^{2+}$-dependent exocytotic machinery (Parpura et al., 1995; Mothet et al., 2005; Parpura and Zorec, 2010), metabolically support and signal to neurons. Hence, the release of gliotransmitters, such as glutamate and metabolic products, such as lactate, can lead to modulation of synaptic transmission and plasticity (Araque et al., 1999a, 1999b; Perea and Araque, 2007; Suzuki et al., 2011). Thus, studying $Ca^{2+}_{cyt}$ and $Na^+_{cyt}$ dynamics is important for understanding the role of astrocytes in physiology of the CNS.

The vast majority of astrocytes in the brain grey matter, together with neurons, endothelial cells and pericytes, represent the neurovascular unit. It is at this interface with blood vessels, which dynamically change their diameter, that astrocytes undergo large morphological changes and mechanical strains associated with changes in their $Ca^{2+}_{cyt}$ (Zonta et al., 2003; Filosa et al., 2004; Mulligan and MacVicar, 2004). Indeed, mechanical stimulation of astrocytes leads to an increase of $Ca^{2+}_{cyt}$ and subsequent release of glutamate (Innocenti et al., 2000; Hua et al., 2004; Montana et al., 2004). Sources of $Ca^{2+}$ for this mechanically induced exocytosis of glutamate from astrocytes have been recently reviewed (Parpura et al., 2011). Briefly, the major source of $Ca^{2+}$ in this process resides within the ER (endoplasmic reticulum) endowed with $InsP_3$ (inositol 1,4,5-trisphosphate) and ryanodine receptors. Activation of these receptors provides a conduit for the release of $Ca^{2+}$ into the cytosol. The ER store depletion and refilling, the latter accomplished by the activity of the store-specific $Ca^{2+}$-ATPase of SERCA (sarcoplasmic/endoplasmic reticulum $Ca^{2+}$-ATPase) type, additionally draws $Ca^{2+}$ from the ECS (extracellular space) via store-operated $Ca^{2+}$ entry. An alternative, albeit less studied conduit for $Ca^{2+}$ entry is associated with the plasma membrane NCX ($Na^+/Ca^{2+}$ exchanger). Activation of ionotropic receptors leading to increases in $Na^+_{cyt}$ and depolarization was reported to stimulate $Ca^{2+}$ entry through the reverse mode of the NCX (Kirischuk et al., 1997). Mild depolarization of astrocytes isolated from adult, but not neonatal, brains led to the reverse mode of NCX operation causing $Ca^{2+}$ entry into astrocytic cytosol and consequential glutamate release (Paluzzi et al., 2007). In this process, however, neither $Na^+_{cyt}$ changes have been investigated, nor the ability of neonatal astrocytes to utilize the reverse mode of NCX due to mechanical stimulation identified.

Astrocytes express the PMCA (plasma membrane: $Ca^{2+}$-ATPase), which extrudes $Ca^{2+}_{cyt}$; NCX which depending of ion concentrations and the plasma membrane potential either extrudes or delivers $Ca^{2+}$ and $Na^+$ to the cytosol; and NKA ($Na^+/K^+$-ATPase) that extrudes $Na^+_{cyt}$. PMCAs are expressed throughout the plasma membrane of astrocytes (Mata and Fink, 1989; Blaustein et al., 2002), while NCXs are enriched at distal processes of astrocytes surrounding synapses (Minelli et al., 2007). A subtype of NKA (type $\alpha 2$) colocalizes with NCX in astrocytes at plasma membrane–ER junctions, a site of 'sodium microdomains' (Juhaszova and Blaustein, 1997; Blaustein et al., 2002).

We studied the contribution of PMCA, NCX and NKA to $Ca^{2+}$ and $Na^+$ homoeostasis in astrocytes isolated from neonatal rat visual cortex, both at rest and when these cells were mechanically stimulated. Our data reveal a complex interplay between these $Ca^{2+}$-handling proteins, with NKA being the major $Na^+$ extruder and PMCA the major $Ca^{2+}$ extruder from astrocytes at rest. Surprisingly, the blockade of these pumps had minor effects on $Ca^{2+}_{cyt}$ and $Na^+_{cyt}$ levels in mechanically stimulated cells. Rather, NCX in the reverse mode was a major contributor to $Ca^{2+}$ and $Na^+$ homoeostasis in mechanically stimulated astrocytes, although it operated also in resting cells. In addition, NCX facilitated mechanically induced $Ca^{2+}$-dependent exocytotic release of glutamate from astrocytes. We propose that the NCX reverse mode, due to location and turnover rate of this transporter, could be linked to the activation of plasmalemmal ionotropic glutamate receptors and glutamate transporters at the tripartite synapse to accomplish fast and spatially localized gliotransmission. Naturally, such intercellular signalling pathway would operate in parallel to a slower and more widely distributed pathway that requires activation of mGluR (metabotropic glutamate receptor) and $Ca^{2+}$ release from the ER in perisynaptic astroglial compartments. Some of these data have appeared in preliminary form (Reyes and Parpura, 2009).

## MATERIALS AND METHODS

### Astrocyte cultures

We grew solitary astrocytes (individual astrocytes devoid of contact with other astrocytes) from visual cortices of 1- to 2- day-old Sprague Dawley rats as previously described (Hua et al., 2004; Reyes and Parpura, 2008). Briefly, visual cortices were dissected and enzymatically treated with papain (20 IU/ml, 1 h at 37°C) in the presence of L-cysteine (0.2 mg/ml); digestion was terminated by trypsin inhibitor (10 mg/ml; type II-O; 5 min at room temperature). Tissue was mechanically dissociated and neural cells were seeded into culture flasks containing culture medium composed of $\alpha$-MEM ($\alpha$-minimum essential medium, without phenol red; Invitrogen) supplemented with fetal bovine serum (10% (v/v); Thermo Scientific HyClone), glucose (20 mM), L-glutamine (2 mM), sodium pyruvate (1 mM), sodium bicarbonate (14 mM), penicillin (100 IU/ml), and streptomycin (100 µg/ml) (pH 7.35). After allowing cells to adhere to the bottom of the flasks for 1 h, they were washed and provided with fresh medium. Cells were then maintained at 37°C in a 95% air/ 5% $CO_2$ incubator for 5–7 days to obtain cell growth and proliferation to approx. 60% confluency. At that juncture, the cell cultures were purified for astrocytes using a previously described procedure (McCarthy and de Vellis, 1980). Purified astrocytes were detached from the flasks using trypsin (10,000

Nα-benzoyl-arginine ethyl ester hydrochloride units/ml; Sigma–Aldrich). After inhibition of trypsin activity by addition of complete culture medium, cells were pelleted using centrifugation ($100 \times g$ for 10 min), resuspended and plated onto round (12 mm in diameter) glass coverslips (Fisher Scientific, cat. no. 12-545-82-12CIR-1D) pre-coated with PEI (polyethyleneimine, 1 mg/ml; Sigma). Purified astrocytes were kept in culture medium at 37 °C in a 95% air/5% $CO_2$ incubator for 5–8 days when used in experiments. The purity of astrocytic culture (>99%) was confirmed: (i) by indirect immunocytochemistry using anti-glial fibrillary acidic protein antibody (Supplementary Figure S1 at http://www.asnneuro.org/an/004/an004e075add.htm) and (ii) by visualization of accumulation of a dipeptide, β-Ala-Lys, conjugated to 7-amino-4-methylcoumarin-3-acetic acid as previously described (Hua et al., 2004; Montana et al., 2004; Malarkey et al., 2008). Astrocytes in our culture system are flat polygonal cells having simplified morphological appearance when compared with astrocytes *in situ* (Supplementary Figure S1) (Hua et al., 2004; Montana et al., 2004; Malarkey et al., 2008).

## Pharmacological agents

Concentration and pre-incubation times for each pharmacological agent were adapted from literature (Goldman et al., 1994; Chaudhary et al., 2001; Benz et al., 2004; Rojas et al., 2007): caloxin 2A1 (peptide sequence VSNSNWPSFPSSGGG-$NH_2$; 2 mM, 5 min; Synthetic Biomolecules), benzamil hydrochloride (benzamil; 100 μM, 5 min; Alexis Biochemical), KB-R7943 (2-[2-[4-(4- nitrobenzyloxy)phenyl]ethyl]isothiourea methane sulfonate; 30 μM, 10 min; EMD Chemicals, Inc.), and ouabain (1 mM, 10 min; Sigma). These agents were delivered to astrocytes in external solution (pH 7.35) containing (in mM): sodium chloride (140), potassium chloride (5), calcium chloride (2), magnesium chloride (2), HEPES (10) and glucose (5). In experiments using mechanical stimulation, and prior to imaging, astrocytes were pre-incubated with solutions containing a pharmacological agent or a combination of them at room temperature (22–25 °C) at prescribed times above, and were then kept bathed in the agent(s) during the entire imaging procedure lasting approx. 250 s for ion measurements; for glutamate measurements, inherent to a dual run approach (see below), the imaging procedure lasted twice as long.

## Intracellular $Ca^{2+}$ imaging

$Ca^{2+}_{cyt}$ levels in somata of cultured solitary astrocytes were assessed using the $Ca^{2+}$ indicator fluo-3 as described earlier (Hua et al., 2004; Montana et al., 2004; Lee et al., 2008). Briefly, astrocytes were loaded with AM (acetoxymethyl) ester of fluo-3 (10 μg/ml; Invitrogen) in external solution containing pluronic acid (0.025% (w/v)) for 30 min at room temperature. To allow de-esterification of fluo-3 AM, cells were subsequently kept in external solution for 30 min at room temperature. Cells were then incubated with pharmacological agents described above. Coverslips were mounted onto a recording chamber, and astrocytes were visualized with a standard FITC filter set (Chroma). Fluorescence intensities obtained from somata of indicator-loaded astrocytes were corrected (digital subtraction) for the background fluorescence measured from regions of coverslips containing no cells. Fluorescence data were expressed as $\Delta F/F_o$ (%) with the cell baseline fluorescence ($F_o$) representing the average of the first five images before mechanical stimulation, while ΔF represents the change in fluorescence emission. The $[Ca^{2+}]_{cyt}$ ($Ca^{2+}_{cyt}$ concentration) was determined using calibration of fluo-3 as described elsewhere (Parpura and Haydon, 2000; Malarkey et al., 2008). In experiments studying the effect of agents on basal $Ca^{2+}_{cyt}$, we expressed fluorescence emission as a ratio of the average background subtracted fluorescence at testing time [*F*; five consecutive images obtained at the end of the incubation time with the agent(s)] over the average baseline fluorescence of cells at rest [$F_o$; five consecutive images obtained just prior to the addition of the agent(s)].

## Intracellular $Na^+$ imaging

$Na^+_{cyt}$ levels in somata of cultured solitary astrocytes were assessed using the $Na^+$ indicator CoroNa$^{TM}$Green AM (10 μM; Invitrogen) (Meier et al., 2006). Astrocytes were loaded with the indicator, imaged, and data collected and processed as described above for $Ca^{2+}$ imaging. Because CoroNa$^{TM}$Green tends to leak out of the cell, its intracellular fluorescence intensity substantially decays over time (Meier et al., 2006). Consequently, using a linear regression and extrapolation of the baseline fluorescence of individual traces, we corrected them for the leak of the dye. To estimate the concentration of intracellular $Na^+$ concentration, we used a calibration protocol *in situ*. Here, astrocytes were imaged in external solution containing various concentrations of $Na^+$ (in mM: 140, 100, 50 or 10). Following approx. 4 min exposure to a particular extracellular $Na^+$ concentration, astrocytes were treated with the $Na^+$ ionophore gramicidin (50 μM; Sigma). On equilibration of the intracellular milieu with the extracellular $Na^+$ concentration by using the peak of CoroNa$^{TM}$Green $\Delta F/F_o$ and by applying an exponential fit ($r = 0.97$) to the data, we obtained the relationship between $[Na^+]_{cyt}$, ($Na^+_{cyt}$, concentration) and CoroNa$^{TM}$Green $\Delta F/F_o$, which can be formulated as: $[Na^+]_{cyt} = 16.597\ mM \times e^{(0.0131 \times \Delta F/Fo)}$.

## Buffering of intracellular $Ca^{2+}$

To buffer $Ca^{2+}_{cyt}$ in astrocytes, during the loading procedure with either fluo-3 AM or CoroNa$^{TM}$Green AM, we co-loaded astrocytes with the $Ca^{2+}$ chelator BAPTA-AM [1,2-bis-(*o*-aminophenoxy)ethane-*N*,*N*,*N*′,*N*′-tetra-acetic acid tetrakis-acetoxymethyl ester]; 100 μM; Invitrogen, followed by a 30 min de-esterification period.

## Extracellular glutamate imaging

$Ca^{2+}$-dependent glutamate release from cultured solitary astrocytes was measured using the L-GDH (glutamate dehydrogenase)-linked assay as previously described (Hua et al., 2004; Montana et al., 2004; Lee et al., 2008). PEI-coated coverslips containing cultured astrocytes were mounted onto a recording chamber and bathed in external solution. A set of images containing the cell of interest were taken in a sham run and used to correct for reduction of fluorescence due to photobleaching in the follow-up experimental run, for which the external solution was exchanged with fresh external solution supplemented with 1 mM of $NAD^+$ (Sigma) and 55–61 IU/ml of GDH (Sigma). Visualization was achieved using a standard DAPI (4′6-diamidino-2-phenylindole) filter set (Nikon). When released, glutamate is oxidized to α-ketoglutarate by GDH, while bath-supplied $NAD^+$ is reduced to NADH, a fluorescent product when excited by UV light. Fluorescence data were expressed as $\Delta F/F_o$ (%) with the baseline fluorescence ($F_o$) being the fluorescence of the medium surrounding the solitary astrocyte, immediately and laterally of its soma, before mechanical stimulation. To account for the possibility that KB-R7943 has an effect on the activity of the GDH in the medium surrounding the astrocytes, a spectrophotometer assay (Genequant Pro) was performed using NADH absorbance as a measure of GDH activity (Reyes and Parpura, 2008; Reyes et al., 2011). The assay solution contained $NAD^+$ (1 mM), glutamate (100 μM), and approx. 59 IU/ml of GDH. The NADH produced from a 5-min reaction was monitored by its absorbance at 320 nm. There was no significant difference (Student's *t*-test, $P=0.09$) in NADH absorbance in assay solution either containing KB-R7943 (30 μM; $n=7$; $0.35 \pm 0.03$) or lacking this agent [control; $n=7$; $0.43 \pm 0.03$ (mean ± SEM)]. It should be noted that due to its fluorescence when excited with UV light, benzamil is not amenable for use in our glutamate release assay.

## Image acquisition and processing

An inverted microscope (TE 300; Nikon), equipped with DIC (differential interference contrast), wide-field fluorescence illumination and oil-immersion objectives, was used in all experiments. For glutamate imaging we used a 40× SFluor objective (1.3 NA; Nikon), whereas all other experiments were done using a 60× Plan Apo objective (1.4 NA; Nikon). Images were acquired using a CoolSNAP-HQ cooled CCD (charge-coupled device) camera (Roper Scientific Inc.) driven by V++ imaging software (Digital Optics Ltd.). All raw data/images had their pixel intensities within the camera's dynamic range (0–4095). For glutamate release analysis, the $\Delta F/F_o$ of the treatment groups were ranked and normalized to accommodate for variations in enzyme-based method and culture conditions, and to allow comparisons between experimental batches, as we previously described (Reyes and Parpura, 2008). Similar rankings of intracellular $Na^+$ and $Ca^{2+}$ dynamics were done for consistency.

## Mechanical stimulation

To stimulate a solitary astrocyte of interest, we employed mechanical contact using a glass pipette filled with external solution as we described in detail elsewhere (Hua et al., 2004). Briefly, this approach allows spatio-temporal control of the stimulus application without affecting plasma membrane integrity. The establishment of the patch pipette contact with the plasma membrane was determined by an increase in pipette resistance monitored using a patch-clamp amplifier (PC-ONE) that delivered −20 mV, 10 ms square pulses at 50 Hz. Once established, cell contact was maintained for approx. 1 s. The strength of the stimulus, expressed as $\Delta R/R_o$ (%), where $R_o$ represents the pipette resistance (1.4–9.3 MΩ) prior to the establishment of a pipette-astrocyte contact, and $\Delta R$ represents the increase in the resistance (0.02–1.3 MΩ) during the contact, had comparable intensities, under all conditions tested (Mann–Whitney *U*-test, $P=0.092$–$0.934$).

## Statistical analysis

All reported effects were tested using data originating from at least three independent cultures. The comparison of the pipette resistance increases ($\Delta R/R_o$) in different conditions were tested by Mann–Whitney *U*-test. Effects of the pharmacological agents on basal and mechanically evoked intracellular $Ca^{2+}$ and $Na^+$ levels were tested using one-way ANOVA, followed by Fisher's LSD (least significant difference) test. Effects of mechanical stimulation on intracellular $Ca^{2+}$ and $Na^+$ levels were assessed with paired *t*-tests. Effects of BAPTA/AM on mechanically induced intracellular $Ca^{2+}$ and $Na^+$ load, as well as that of KB-R7943 on $Ca^{2+}$ accumulation and glutamate release were tested using Mann–Whitney *U*-test. Data are expressed as means ± SEM.

# RESULTS

## PMCA, NCX and NKA regulate basal $Ca^{2+}_{cyt}$ and $Na^+$ levels in cultured cortical astrocytes

PMCA, NCX and NKA have been shown to jointly regulate $Ca^{2+}_{cyt}$ and $Na^+_{cyt}$ homoeostasis at neuronal presynaptic terminals (Regehr, 1997; Zhong et al., 2001). Since astrocytes exhibit spatio-temporal changes in $[Ca^{2+}]_{cyt}$ (Verkhratsky et al., 1998) and $[Na^+]_{cyt}$ (Kirischuk et al., 1997; Rose and Ransom, 1997; Kirischuk et al., 2007), it has been proposed that combined PMCA, NCX and NKA also contribute to the regulation of astrocytic $[Ca^{2+}]_{cyt}$ and $[Na^+]_{cyt}$ (Goldman et al., 1994; Blaustein et al., 2002). Consequently, we evaluated the contribution of PMCA, NCX and NKA in maintaining the basal $Ca^{2+}_{cyt}$ and $Na^+_{cyt}$ levels in cultured astrocytes using specific pharmacological inhibitors previously tested in non-neuronal/glial cell types.

We tested the role of the PMCA in preserving basal $[Ca^{2+}]_{cyt}$ by incubating cortical astrocytes with caloxin 2A1 (2 mM; 5 min), a peptide blocker that has affinity for the second extracellular domain sequence of the PMCA (Chaudhary et al., 2001; De Luisi and Hofer, 2003; Kawano et al., 2003). To assess the NCX contribution to basal $Na^+_{cyt}$ and $Ca^{2+}_{cyt}$ regulation, we incubated astrocytes with either the general NCX blocker, benzamil (100 μM; 5 min) or the NCX reverse mode blocker KB-R7943 (30 μM; 10 min) (Benz et al., 2004; Rojas et al., 2004; Rojas et al., 2007). To test the role of NKA in the regulation of basal $[Na^+]_{cyt}$ we used the NKA blocker ouabain (1 mM; 10 min) (Goldman et al., 1994).

We monitored fluo-3 fluorescence to assess changes in basal $[Ca^{2+}]_{cyt}$ in solitary astrocytes. We acquired the resting $Ca^{2+}_{cyt}$ level from astrocytes bathed in external solution, which was then replaced by a pharmacological agent(s) containing solution. In control, astrocytes were sham treated by exchanging the plain external solution. We found that astrocytes treated with caloxin 2A1 showed a significant increase in the basal fluo-3 fluorescence when compared with control, sham-treated, astrocytes (Figure 1A; one-way ANOVA, followed by Fisher's LSD test; $P<0.01$). In contrast astrocytes treated with KB-R7943 or ouabain showed a significant decrease in fluo-3 fluorescence (Figure 1A; one-way ANOVA, followed by Fisher's LSD test; $P<0.01$). These changes in fluo-3 fluorescence corresponded to rather subtle variations in calculated $[Ca^{2+}]_{cyt}$ from approx. 73 nM at rest, before the treatment with an agent, to approx. 85 nM in caloxin 2A1, approx. 61 nM in KB-R7943 and approx. 58 nM in ouabain; the exchange of external solution alone in sham-treated astrocytes resulted in basal $[Ca^{2+}]_{cyt}$ of approx. 77 nM, which was essentially unchanged from the resting level. In addition, astrocytes treated with benzamil did not exhibit significant change in fluorescence when compared with control. Furthermore, we incubated astrocytes with various agents in tandem. We found that astrocytes treated with the caloxin 2A1/benzamil or benzamil/ouabain combination did not exhibit significant changes in fluo-3 fluorescence, while astrocytes treated with caloxin 2A1/ouabain showed a significant increase in fluorescence, corresponding to $[Ca^{2+}]_{cyt}$ of approx. 82 nM, when compared with control (Figure 1A; one-way ANOVA, followed by Fisher's LSD test; $P<0.05$).

Plasmalemmal NCX regulates both $[Ca^{2+}]_{cyt}$ and $[Na^+]_{cyt}$ depending on the relative concentration of these two ions and the plasma membrane potential (Goldman et al., 1994; Rojas et al., 2007). Similar to their differential effect on $[Ca^{2+}]_{cyt}$, benzamil and KB-R7943 had a differential effect on the $[Na^+]_{cyt}$. Astrocytes treated with benzamil did not show a significant difference in CoroNa$^{TM}$Green fluorescence, corresponding to approx. 19.0 mM of $[Na^+]_{cyt}$, when compared with levels (approx.16.6 mM) recorded in astrocytes at rest or sham-treated. Treatment of these cells with KB-R7943 caused a decrease in CoroNa$^{TM}$Green fluorescence corresponding to approx. 11.3 mM of $[Na^+]_{cyt}$ (Figure 1B; one-way ANOVA, followed by Fisher's LSD test; $P<0.01$). Since PMCA does not transport $Na^+$, as predicted, astrocytes treated with caloxin 2A1 did not exhibit a change in $[Na^+]_{cyt}$, as evident from the lack of change in CoroNa$^{TM}$Green fluorescence compared with the sham-treated control. Furthermore, since the NKA transports $Na^+$ extracellularly, astrocytes treated with ouabain exhibited significant increase in $[Na^+]_{cyt}$, corresponding to approx. 24.1 mM, when compared with control (Figure 1B; one-way ANOVA, followed by Fisher's LSD test; $P<0.01$). Astrocytes treated with benzamil in conjunction with ouabain exhibited a significant increase in CoroNa$^{TM}$Green fluorescence (corresponding to approx. 34.7 mM of $[Na^+]_{cyt}$), while astrocytes treated with caloxin 2A1 in conjunction with ouabain exhibited a significant decrease in fluorescence (corresponding to approx. 8.3 mM of $[Na^+]_{cyt}$) when compared with control (Figure 1B; one-way ANOVA, followed by Fisher's LSD test; $P<0.01$).

Taken together, at resting conditions it appears that the PMCA is the primary astrocytic $Ca^{2+}$ extruder, since blockage

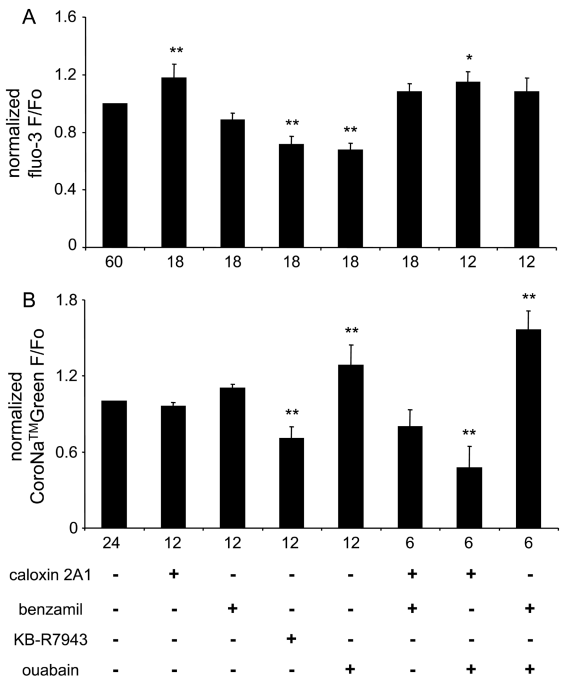


**Figure 1 PMCA, NCX and NKA modulate basal $Ca^{2+}_{cyt}$ and $Na^+_{cyt}$ levels in neonatal solitary cortical astrocytes at rest**

(**A**) Normalized fluo-3 fluorescence, reporting on $Ca^{2+}_{cyt}$ levels, in astrocytes at rest. Astrocytes treated with caloxin 2A1 (PMCA blocker) alone or in conjunction with ouabain (NKA blocker) showed a significant increase in basal $Ca^{2+}_{cyt}$ levels, which were decreased when cells were treated with KB-R7943 (NCX reverse mode blocker) or ouabain. (**B**) Normalized CoroNa$^{TM}$Green fluorescence, reporting on $Na^+_{cyt}$ levels, in astrocytes at rest. A significant increase in basal $Na^+_{cyt}$ levels was recorded from astrocytes treated with ouabain alone or in combination with benzamil (general NCX blocker), while astrocytes treated with KB-R7943 or caloxin 2A1/ouabain combination exhibited a decrease in basal $Na^+_{cyt}$ levels. Bars represent average (±SEM) of fluorescence ratio before ($F_o$) and after ($F$) incubation of astrocytes in various agents. Statistical comparisons were made between time-matched sham treated (control) and agent treated astrocytes (one-way ANOVA, followed by Fisher's LSD test; *$P<0.05$, **$P<0.01$), whose numbers in each group are given below abscissas.

by caloxin 2A1 caused a significant increase in $[Ca^{2+}]_{cyt}$. In contrast, at resting conditions the NCX appears to facilitate $Ca^{2+}$ entry to the astrocytic cytosol, thus operating in the reverse mode, detected as the reduction of fluo-3 fluorescence in astrocytes treated with KB-R7943. The primary astrocytic $Na^+$ extruder appears to be NKA, since its inhibition by ouabain caused significant increase in astrocytic $[Na^+]_{cyt}$.

## Mechanical stimulation causes both $Ca^{2+}$ and $Na^+$ cytosolic increases in astrocytes

Solitary astrocytes are known to respond to mechanical stimulation, which does not compromise the plasma membrane integrity, by increasing their intracellular $Ca^{2+}$ levels (Hua et al., 2004). The majority of mechanically induced $Ca^{2+}_{cyt}$ accumulation originates from the ER internal store, although plasmalemmal $Ca^{2+}$ entry contributes to this excitability and is ultimately required for the (re)filling of ER $Ca^{2+}$ stores, a process that involves store-operated $Ca^{2+}$ entry via TRPC (canonical transient receptor potential) 1 channels (Hua et al., 2004; Malarkey et al., 2008); these channels are permeable for both $Ca^{2+}$ and $Na^+$, albeit with much higher $Ca^{2+}$ permeability (Clapham, 2003; Rychkov and Barritt, 2007). Additionally, mitochondria modulate the magnitude of this mechanically induced excitability (Reyes and Parpura, 2008). However, whether mechanical stimulus can also affect $Na^+_{cyt}$ loads that should be inherently linked to $Ca^{2+}_{cyt}$ changes has not been determined yet.

To address this issue, we loaded astrocytes, in parallel, with either fluo-3 or CoroNa$^{TM}$Green. As expected, mechanical stimulus caused a typical increase in $Ca^{2+}_{cyt}$ levels in solitary astrocytes characterized by an initial transient $Ca^{2+}$ elevation followed by a slowly decaying response (Figure 2A, paired *t*-test, $P<0.01$). Two aspects of the $Ca^{2+}_{cyt}$ kinetics in astrocytes due to mechanical stimulation were measured and analysed: the peak and cumulative $Ca^{2+}$ responses. The peak response represents the maximum $Ca^{2+}_{cyt}$ in the stimulated astrocyte as a result of $Ca^{2+}$ entry into the cytosol from the ER store and ECS, while the cumulative response additionally represents the declining $Ca^{2+}_{cyt,}$ as free $Ca^{2+}$ is removed from cytosol by pumps, such as the PMCA and SERCA (Kim et al., 2005; Reyes and Parpura, 2008). Mitochondria modulate the peak of $[Ca^{2+}]_{cyt}$ transient as they immediately sequester $Ca^{2+}$, while during the decay phase they slowly release $Ca^{2+}$. In addition to inducing the $Ca^{2+}$ response, mechanical stimulation caused an increase in intracellular $Na^+$ levels (Figure 2D; paired *t*-test, $P<0.01$). Similar to the $Ca^{2+}$ response, the mechanically induced $Na^+$ response included an initial transient increase followed by a slow decline, albeit the overall response had a slower time-course than that of mechanically induced $[Ca^{2+}]_{cyt}$ transient.

Such coordinated dynamics, where $Na^+_{cyt}$ changes appear to follow those of $Ca^{2+}_{cyt}$, raised the question of whether the mechanically induced $Na^+$ response involves NCX activity. Since the amount of $Na^+_{cyt}$ extruded by NCXs is proportional

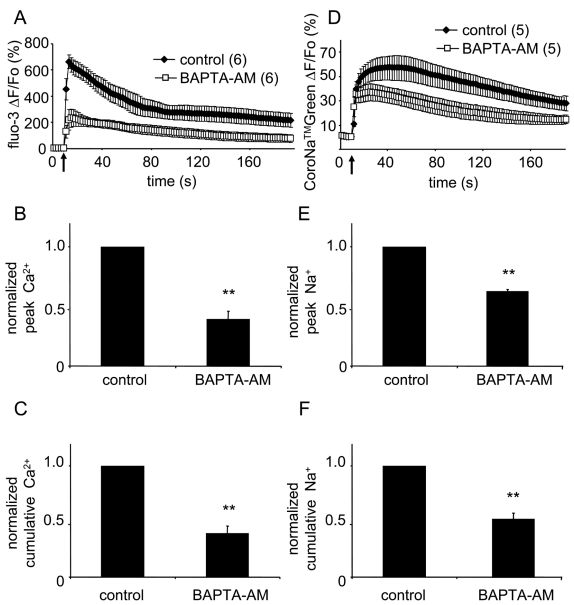


**Figure 2 Mechanical stimulation of astrocytes induces both $Na^+_{cyt}$ and $Ca^{2+}_{cyt}$ signals**

(**A**) Average kinetics of fluo-3 fluorescence, reporting on changes in $Ca^{2+}_{cyt}$, in solitary astrocytes that were mechanically stimulated. (**B**, **C**) Bar graphs showing normalized peak and cumulative $Ca^{2+}_{cyt}$ responses, respectively. (**D**) Average kinetics of CoroNa$^{TM}$Green, reporting on changes in $Na^+_{cyt}$, in mechanically stimulated solitary astrocytes. (**E**, **F**) Bar graphs showing normalized peak and cumulative $Na^+_{cyt}$ responses, respectively. Mechanical stimulation evoked both $Ca^{2+}_{cyt}$ and $Na^+_{cyt}$ increases (**A** and **D**, receptively). Peak and cumulative values of mechanically induced $Ca^{2+}_{cyt}$ elevations were greatly reduced when cells were pre-incubated with the $Ca^{2+}$ chelator BAPTA-AM (**B** and **C**, respectively). Similar reduction in peak and cumulative values of $Na^+_{cyt}$ elevations was observed in astrocytes treated with BAPTA/AM (**E** and **F**, respectively). Points and bars represent means ± SEM of measurements. Arrows in **A** and **D** indicate the time when the pipette-astrocyte contact occurred. Numbers in parentheses indicate the number of cells in each group. Asterisks denote significant change in comparison with control, untreated and stimulated, astrocytes (Mann–Whitney *U*-test; $^{**}P<0.01$).

to the amount of extracellular $Ca^{2+}$ taken in, if the reverse operation of the NCX could play a role in mechanically induced $Ca^{2+}$ and $Na^+$ dynamics in astrocytes, we predict that the buffering of $Ca^{2+}_{cyt}$, an experimental manipulation that would facilitate the reverse mode (see Discussion), could result in a decrease of $Na^+$ load in these cells. In contrast, a sole involvement of TRPC1 in mechanically induced $Ca^{2+}$ and $Na^+$ dynamics under conditions of $Ca^{2+}_{cyt}$ buffering should not lead to a decrease, but rather to an increase in $Na^+$ load. To test this hypothesis, we used the $Ca^{2+}$ chelator BAPTA-AM (100 μM; 30 min) to co-load astrocytes with one of the above indicators, while cells loaded with indicators alone served as control. Mechanically stimulated astrocytes co-loaded with the $Ca^{2+}$ chelator exhibited a decrease in peak and cumulative fluo-3 (Figures 2A–2C) and CoroNa$^{TM}$Green (Figure 2D–2F) fluorescence when compared with control cells (Mann–Whitney *U*-test, $P<0.01$). These data point to a role of NCX reverse mode in modulation of mechanically

induced $Ca^{2+}$ and $Na^+$ dynamics in astrocytes, which we further studied using a pharmacological approach below.

## PMCA, NCX and NKA modulate mechanically induced $Ca^{2+}_{cyt}$ accumulations in astrocytes

Having determined effects of pharmacological blockers of PMCA, NCX and NKA on $Ca^{2+}$ and $Na^+$ cytosolic levels of cells at rest along with finding that mechanical stimulation induced both $Ca^{2+}_{cyt}$ and $Na^+_{cyt}$ elevations, we studied the role of these pumps and the exchanger on cytosolic $Ca^{2+}$ dynamics of mechanically stimulated astrocytes. As we described above, mechanical stimulation of control astrocytes caused a robust increase in $[Ca^{2+}]_{cyt}$, corresponding to approx. 3.8 μM (Figure 3A; paired *t*-test, $P<0.01$). We found that the treatment of astrocytes with either caloxin 2A1 (2 mM; 5 min) to block PMCAs, benzamil (100 μM; 5 min) to block NCX, or ouabain (1 mM; 10 min) to block NKA modulated the mechanically induced $Ca^{2+}$ response as evident in the average kinetics of the fluorescence intensity (Figure 3A). We should be reminded that pharmacological agents affect resting $Ca^{2+}_{cyt}$ levels bringing them to various post-treatment baselines (Figure 1A). Since we were interested in the astrocytic ability to handle $Ca^{2+}_{cyt}$ after the treatments, we used post-treatment $Ca^{2+}_{cyt}$ levels as a baseline ($F_o$) for further quantitative analysis. Here, pretreatment of astrocytes with either caloxin 2A1, benzamil or ouabain reduced the peak of mechanically induced $Ca^{2+}$ response, when compared with control (Figure 3B; one-way ANOVA, followed by Fisher's LSD test; $P<0.01$ for caloxin 2A1 and benzamil, while $P<0.05$ for ouabain). In contrast, astrocytes treated with caloxin 2A1 did not exhibit significant difference in cumulative response, while cells treated with benzamil or ouabain exhibited attenuated or enhanced cumulative responses respectively (Figure 3C, one-way ANOVA, followed by Fisher's LSD test; $P<0.01$).

Taken together it appears that PMCA, NCX and NKA all play a role in modulating the mechanically induced $Ca^{2+}$ entry into the cytosol since these agents attenuated the peak $Ca^{2+}$ response. In addition, it also appears that NCX and NKA play additional, but opposing roles in the removal of $Ca^{2+}$ from the cytosol.

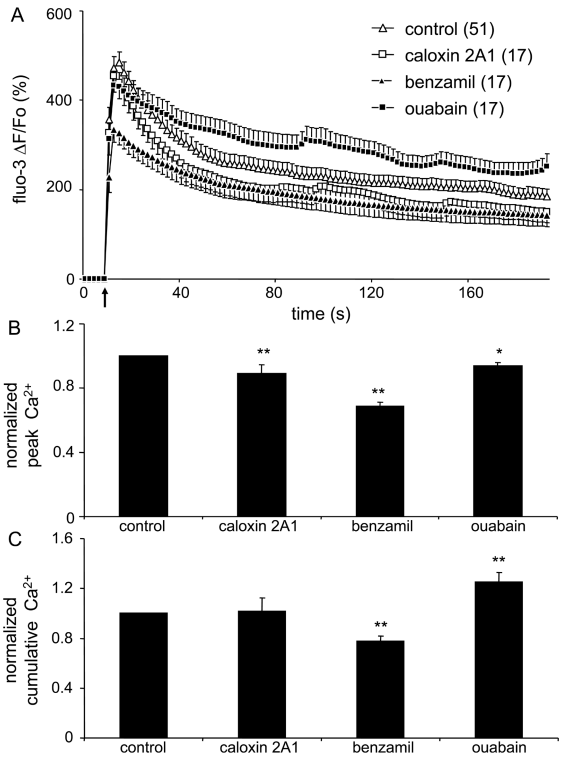


**Figure 3 $Ca^{2+}_{cyt}$ accumulation in astrocytes induced by mechanical stimulation is modulated by the plasmalemmal PMCA, NCX, and NKA**

(**A**) Average kinetics of fluo-3 fluorescence, reporting on changes in $Ca^{2+}_{cyt}$, in solitary astrocytes treated with pharmacological agents and in response to mechanical stimulation. Arrow represents the time when mechanical stimulation was applied to the cells. (**B**,**C**) Bar graphs showing normalized peak and cumulative $Ca^{2+}_{cyt}$ responses, respectively. When treated with caloxin 2A1, benzamil and ouabain, mechanically stimulated astrocytes had a decrease in the peak $Ca^{2+}_{cyt}$ response (**B**). Benzamil led to a decrease, while ouabain to an increase in the normalized cumulative $Ca^{2+}_{cyt}$ response obtained from mechanically stimulated astrocytes (**C**). Points and bars represent means ± SEM of measurements from solitary astrocytes (numbers in parentheses); SEM are shown in single directions for clarity. Asterisks denote significant change in comparison with control group (one-way ANOVA, followed by Fisher's LSD test; *$P<0.05$, **$P<0.01$).

## $Na^+_{cyt}$ load induced by mechanical stimulation is mediated by NCX

Mechanical stimulation of control astrocytes, in addition to $Ca^{2+}_{cyt}$ response, caused an increase in $[Na^+]_{cyt}$ corresponding to ~36.8 mM (Figure 4A; paired *t*-test, $P<0.01$), which is about the same $[Na^+]_{cyt}$ reached upon treatment of astrocytes at rest with the NKA blocker (Figure 1B). We tested whether mechanically induced $Na^+$ load in astrocytes can be modulated by NCX and NKA. We loaded cortical astrocytes with CoroNa$^{TM}$Green, and then treated them with either benzamil (100 μM; 5 min) to block NCX, or ouabain (1 mM; 10 min) to block NKA. We were interested in the astrocytic ability to handle $Na^+_{cyt}$ following pharmacological treatments, which affected resting $[Na^+]_{cyt}$ levels bringing them to various post-treatment baselines (Figure 1B). Thus, we used post-treatment $[Na^+]_{cyt}$ baselines for further quantitative analysis. Astrocytes pretreated with benzamil showed a reduced mechanically induced peak and cumulative CoroNa$^{TM}$Green fluorescence (Figures 4A and 4B; one-way ANOVA, followed by Fisher's LSD test; $P<0.01$), while ouabain did not significantly affect these parameters by comparison to control astrocytes. Additionally, when ouabain was added in combination with benzamil, it did not alter the effect caused by benzamil (Figures 4B–4C).

Thus, it appears that the NCX may contribute to $Na^+$ entry into cytosol of mechanically stimulated astrocytes since its blockade with benzamil reduced the $Na^+$ load in stimulated astrocytes. In contrast, the NKA appears to be a minor player in the extrusion of $Na^+$ in mechanically stimulated astrocytes.

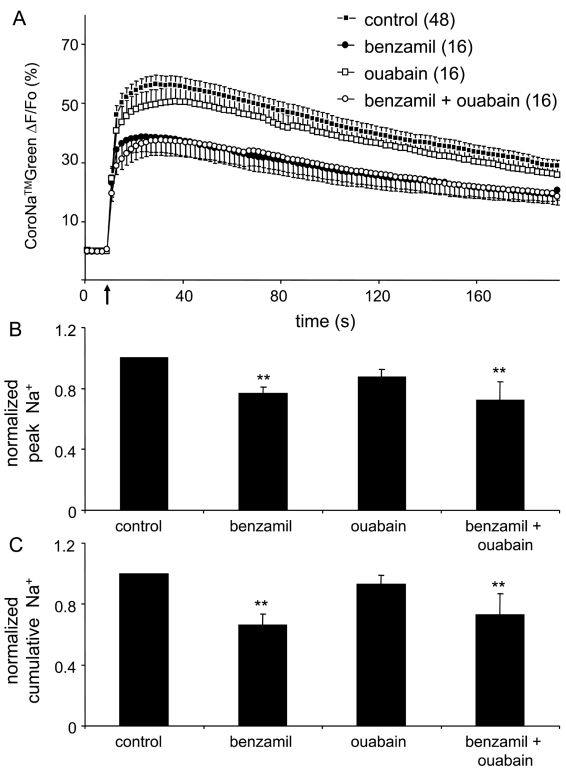


**Figure 4 $Na^{+}_{cyt}$ accumulation in astrocytes induced by mechanical stimulation is regulated by the plasmalemmal NCX**

(**A**) Average kinetics of CoroNa™Green fluorescence, reporting on changes in $Na^{+}_{cyt}$, in solitary astrocytes treated with pharmacological agents and in response to mechanical stimulation. Arrow represents the time when mechanical stimulation was applied to the cells. (**B**, **C**) Bar graphs showing normalized peak and cumulative $Na^{+}_{cyt}$ values of mechanically stimulated astrocytes, respectively. Mechanically stimulated astrocytes pre-treated with benzamil alone or in combination with ouabain had a significantly lower peak $Na^{+}_{cyt}$ values when compared with control cells (**B**). These treatments caused a similar decrease in normalized cumulative $Na^{+}_{cyt}$ values (**C**). Ouabain had no effect on either a peak or cumulative response. Points and bars represent means ± SEM of measurements from solitary astrocytes (numbers in parentheses); SEM are shown in single directions for clarity. Asterisks denote significant change in comparison with control group (one-way ANOVA, followed by Fisher's LSD test; $^{**}P<0.01$).

## Mechanically induced glutamate release from astrocytes is modulated by the $Ca^{2+}$ entry via the reverse mode of NCX

Benz et al. (2004), using benzamil, showed that the NCX participates in $Ca^{2+}$ signalling, and in the subsequent release of homocysteic acid from cortical astrocytes stimulated by glutamate. Additionally, activation of astroglial ionotropic receptors causing increases in $[Na^{+}]_{cyt}$ and depolarization engaged this exchanger in the reverse mode to cause $Ca^{2+}$ entry (Kirischuk et al., 1997; Rojas et al., 2007). Similarly, mild depolarization, due to an increase in extracellular $K^{+}$ (15 and 35 mM), of cortical astrocytes cultured from adult, but not neonatal, rats caused NCX to operate in the reverse mode and generated $[Ca^{2+}]_{cyt}$ increases which triggered release of glutamate (Paluzzi et al., 2007); these effects were blocked by KB-R7943 implicating the reverse mode of NCXs. Consequently, using KB-R7943, we investigated whether the reverse mode of NCX can contribute to mechanically induced $Ca^{2+}$-dependent exocytosis of glutamate from neonatal astrocytes.

Astrocytes were loaded, in parallel, with either the $Ca^{2+}$ indicator fluo-3 or the $Na^{+}$ indicator CoroNa™Green. Once again the mechanical stimulus caused increases in $[Ca^{2+}]_{cyt}$ and $[Na^{+}]_{cyt}$ levels, corresponding to approx. 4.2 μM and 47.3 mM respectively (Figures 5A and 5D; paired *t*-test, $P<0.01$) When we blocked $Ca^{2+}$ entry via the reverse mode of NCX with KB-R7943 (30 μM; 10 min), we saw a significant decrease in the mechanically evoked $Ca^{2+}$ and $Na^{+}$ responses (Figures 5B–5C and 5E–5F respectively; Mann–Whitney *U*-test, $P<0.01$).

To test whether this decrease in mechanically induced $Ca^{2+}$ elevations lead to a reduction of the consequent exocytotic glutamate release from solitary astrocytes we optically monitored the release of glutamate into the ECS surrounding cultured astrocytes using a GDH-linked assay based on accumulation of the fluorescent product, NADH (Hua et al., 2004). Mechanical stimulation of astrocytes caused glutamate release as indicated by a transient increase in NADH fluorescence, reporting on extracellular glutamate levels, corresponding to approx. 0.7 μM, around the astrocytes (Figure 5G; paired *t*-test; $P<0.01$). Incubating astrocytes with KB-R7943 (30 μM; 10 min) reduced the peak and cumulative amount of glutamate released from mechanically stimulated astrocytes (Figure 5H–5I; Mann–Whitney *U*-test, $P<0.01$), indicating that $Ca^{2+}$ entry through NCX is important for the elevation of cytoplasmic $[Ca^{2+}]_{cyt}$ necessary for mechanically induced $Ca^{2+}$-dependent glutamate release from astrocytes.

## DISCUSSION

We studied the role of PMCA, NCX and NKA in coordinated regulation of $Ca^{2+}_{cyt}$ and $Na^{+}_{cyt}$ in astrocytes at rest and upon mechanical stimulation. This stimulus activates major intracellular signalling pathways represented by intracellular $Ca^{2+}$ increase and consequential glutamate release, which is mediated by exocytosis, since Rose Bengal, an inhibitor of vesicular glutamate uptake, abolishes it (Montana et al., 2004); additionally, this stimulus promotes vesicular fusions (Malarkey and Parpura, 2011). $Ca^{2+}$-dependent exocytotic glutamatergic gliotransmission can modulate synaptic transmission and plasticity at the tripartite synapse (Araque et al., 1999c; Perea et al., 2009; Parpura and Zorec, 2010). Since TRPC1 channels, found to be a component of vertebrate mechanosensitive cation channels (Maroto et al., 2005), provide the conduit for $Ca^{2+}$ entry from the ECS (Malarkey et al., 2008), mechanical stimulation could therefore mimic a physiological event, perhaps at astrocyte–blood vessel interface (Reyes et al., 2011). Astrocytes control microcirculation, a process that includes astrocytic $Ca^{2+}$ dynamics

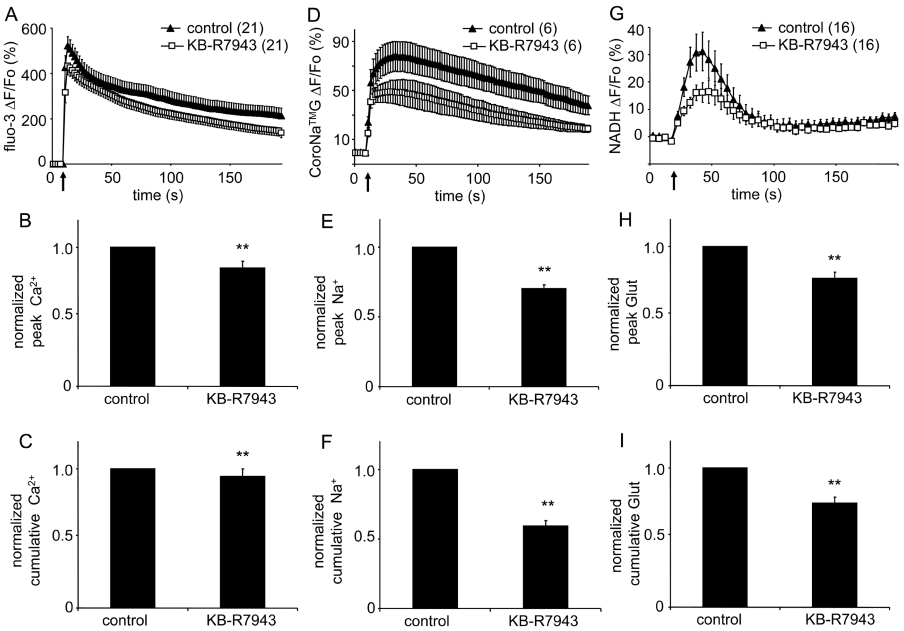


**Figure 5** **Mechanically induced glutamate release from astrocytes is modulated by the $Ca^{2+}$ entry via the reverse mode of the plasmalemmal NCX**

(**A**) Average kinetics of fluo-3 fluorescence, reporting on changes in $Ca^{2+}_{cyt}$, in solitary astrocytes treated with KB-R7943 in response to mechanical stimulation. (**B**, **C**) Bar graphs showing normalized peak and cumulative $Ca^{2+}_{cyt}$ values of mechanically stimulated astrocytes, respectively. When treated with KB-R7943, astrocytes had significantly lower peak and cumulative $Ca^{2+}_{cyt}$ responses to mechanical stimulation than those recorded in control. (**D**) Average kinetics of CoroNa™Green (CoroNa™G) fluorescence, reporting on changes in $Na^+_{cyt}$, in solitary astrocytes treated with KB-R7943 in response to mechanical stimulation. (**E**, **F**) Bar graphs showing normalized peak and cumulative $Na^+_{cyt}$ values of mechanically stimulated astrocytes, respectively. When treated with KB-R7943, astrocytes had significantly lower peak and cumulative $Na^+_{cyt}$ responses to mechanical stimulation than those recorded in control. (**H**) Time lapse of extracellular NADH fluorescence, reporting on glutamate levels in the ECS surrounding somata of solitary astrocytes. Mechanical stimulation of solitary astrocytes caused glutamate release, which was affected by KB-R7943. (**H**, **I**) Normalized peak and cumulative extracellular glutamate (Glut) values of mechanically stimulated astrocytes, respectively. When treated with KB-R7943, astrocytes had both parameters significantly reduced. Points and bars represent means ± SEM of measurements from solitary astrocytes (numbers in parentheses); SEM in A are shown in single directions for clarity. Arrows in **A**, **D** and **G** represent the time when mechanical stimulation was applied to the cells. Asterisks denote significant change in comparison with control group (Mann–Whitney *U*-test, ** $P<0.01$).

occurring at their end feet and bodies (Gordon et al., 2007); it is at this interface that astrocytes undergo large mechanical dynamics.

We used a culturing method yielding solitary astrocytes which appear as flat polygonal cells, having less complex morphological features than astrocytes *in situ* which display elaborate processes and are in intimate contact with other neural cell types. While this system minimizes effects of intercellular astrocyte–astrocyte communications and thus eases the interpretation of our measurements, it brings some limitations. Hence, we were not able to study: (i) the difference in measurements at the somatic region compared with peripheral astrocytic processes, and (ii) the effects that the presence of other cell types, e.g., neurons, would have on our measurements. Nonetheless, using solitary astrocytes we are poised to study in detail spatio-temporal characteristics of $Ca^{2+}$ and $Na^+$ fluxes at mitochondrial, ER and plasma membranes, as well as to assess concentrations of these ions within mitochondria and ER. Indeed, some future studies would also need to cross-correlate our findings in culture with experiments done in more intact systems.

Our finding that mechanical stimulus leads to activation of another intracellular signalling pathway, an increase in $[Na^+]_{cyt,}$ has important consequences to astrocytic metabolism. $Na^+$ entry drives glutamate uptake through the plasma membrane glutamate transporters, and is used to counter transport $H^+$ out of the cytosol via the $Na^+/H^+$ exchanger to regulate cytosolic pH (Deitmer, 2004). As such, maintenance of the $Na^+$ gradient via the NKA is a major ATP expenditure in astrocytes. $Na^+_{cyt}$ increases leading to depolarization due to activity of plasma membrane glutamate transporters (Rojas et al., 2007) and ionotropic glutamate receptors and/or purinoceptors (Benz et al., 2004; Lalo et al., 2006; Lalo et al., 2008) can trigger intracellular $Ca^{2+}$ signalling mediated via NCX. Additionally, increases in $[Na^+]_{cyt}$ can trigger aerobic glycolysis leading to lactate production (Magistretti, 2006), which shuttled to neurons appears to be important for synaptic transmission and plasticity (Suzuki et al., 2011).

Inhibition of the PMCA with caloxin 2A1 raised basal $[Ca^{2+}]_{cyt}$ in cortical astrocytes (Figure 1A). This observation further supports the notion that the PMCA is an important extrusion mechanism to maintain resting levels of $Ca^{2+}$ in

cortical astrocytes, consistent with findings in other cell types, e.g. in mammalian photoreceptors (Morgans et al., 1998) and the calyx of Held (Kim et al., 2005), as well as an invertebrate model of squid giant axons (DiPolo and Beauge, 1979). The relative contribution of PMCA isoforms 1, 2 and 4, expressed by cortical astrocytes (Fresu et al., 1999), in this process is not presently understood and it should be investigated in future. Nonetheless, at stimulated conditions when the $[Ca^{2+}]_{cyt}$ is increased due to $Ca^{2+}$ mobilization from the ER and ECS, inhibition of the PMCA resulted in a significant reduction in the peak and with no effect on the cumulative $Ca^{2+}$ response (Figures 3A and 3B). This apparent lack of the PMCA activity in the removal of $Ca^{2+}{}_{cyt}$ during times of high $[Ca^{2+}]_{cyt}$ indicates that this task is accomplished by other extrusion systems, perhaps the ER store-specific $Ca^{2+}$-ATPase (Hua et al., 2004).

Astrocytes at rest treated with benzamil alone showed only a trend in a $[Ca^{2+}]_{cyt}$ decrease, while application of this general NCX blocker in conjunction with caloxin 2A1 occluded the action of this PMCA blocker, as evidenced by the absence of significant change in $[Ca^{2+}]_{cyt}$ from controls (Figure 1A). This finding suggests that the $Ca^{2+}$ influx via NCX is opposed/balanced by the $Ca^{2+}$ efflux via the PMCA (Figure 1A). This inference is supported by experiments using the specific antagonist of the NCX reverse mode, KB-R7943, which significantly decreased $[Ca^{2+}]_{cyt}$ in cortical astrocytes (Figure 1A), confirming the apparent $Ca^{2+}$ entry via NCX in astrocytes at rest. Additionally, KB-R7943 significantly decreased basal $[Na^{+}]_{cyt,}$ which is likely an indirect effect due to an increased NKA activity. These data also imply that the resting membrane potential in our cultured cortical astrocytes is slightly depolarized from the equilibrium potential for the NCX ($E_{NCX}$), as supported by the previously published work and the calculated $E_{NCX}$. Hence, the membrane potential of cortical astrocytes was reported to have a bimodal distribution with peaks at −68 mV and −41 mV [see Figure 2A of (Kucheryavykh et al., 2007)]. Using our recorded $[Na^{+}]_{cyt}$ of 16.6 mM and $[Ca^{2+}]_{cyt}$ of 73 nM in astrocytes at rest, together with concentration of these ions in the external solution and presumed NCX 3:1 stoichiometry, we calculated $E_{NCX}$ to be approx.−98 mV at 25°C. Thus, the vast majority or astrocytes at rest should display the reverse mode of NCX operation in our experimental conditions. It should be noted that there are three NCX isoforms (1–3), with NCX1 being a predominant isoform, having three splice variants, in primary cultures of rat cortical astrocytes (He et al., 1998). Future experiments are needed to address relative contribution of each of these splice variants in $Ca^{2+}{}_{cyt}$ regulation.

When cortical astrocytes were mechanically stimulated to raise $[Ca^{2+}]_{cyt}$, this stimulus also caused large increases in $[Na^{+}]_{cyt}$. As above by using our recorded peak $[Na^{+}]_{cyt}$ of 36.8 mM and peak $[Ca^{2+}]_{cyt}$ of 4 μM due to mechanical stimulation, we calculated $E_{NCX}$ to be approx.−57 mV at 25°C. Such shift in $E_{NCX}$ would be less favourable for the reverse mode of NCX operation in astrocytes. Consequently, to initially test a possible involvement of NCX in $[Ca^{2+}]_{cyt}$ and $[Na^{+}]_{cyt}$ regulation at elevated levels of these ions, we used BAPTA-AM to clamp the $Ca^{2+}{}_{cyt}$ increase due to mechanical stimulation, corresponding to approx. 614 nM, which would substantially shift $E_{NCX}$ to hyperpolarization at approx. −105 mV assuming unchanged peak $[Na^{+}]_{cyt}$ of 36.8 mM. Such experimental conditions would result in bettering of NCX activity that will be seen as a reduction of $[Na^{+}]_{cyt}$ in astrocytes. Indeed, in BAPTA-AM treated and mechanically stimulated astrocytes we recorded a significantly lower increase of $[Na^{+}]_{cyt}$, approx. 26.8 mM, when compared with controls, at which juncture cells would settle for their $E_{NCX}$ at approx. −80 mV (Figure 2). Of course, large $Ca^{2+}$ entry associated with the reverse mode of NCX operation was clamped down by the fast buffering capabilities of BAPTA, resulting in reduced $Ca^{2+}{}_{cyt}$ levels. We tested this immediate conclusion based on thermodynamics considerations further by using NCX pharmacological blockers.

When cortical astrocytes were mechanically stimulated to raise $[Ca^{2+}]_{cyt}$, inhibition of the NCX with benzamil resulted in a significant reduction in peak and cumulative $Ca^{2+}{}_{cyt}$ accumulation (Figure 3). This observation suggests that the NCX mediates $Ca^{2+}$ entry and promotes $Ca^{2+}$ excitability in astrocytes, consistent with earlier studies (Kirischuk et al., 1997; Benz et al., 2004; Rojas et al., 2007). Since calculated $E_{NCX}$ is approx.−57 mV during the initial phase of mechanical stimulation, depolarization of the majority of astrocytes would be required for the reverse mode of NCX operation. This seems a plausible scenario because mechanical stimulation leads to rather large $Na^{+}{}_{cyt}$ load, which would lead to depolarization of astrocytes. Perhaps as in basal conditions, a decrease in $[Na^{+}]_{cyt}$ that was recorded from mechanically stimulated astrocytes exposed to benzamil could be due to increased activity of NKA (Figure 4), although another alternative is possible (see below). $Ca^{2+}$ entry through the NCX may modulate the $InsP_3$ receptor-gated channel activation, since the NCX1 isoform can associate with plasma membrane–ER junctions, microdomains containing $InsP_3$ receptors (Lencesova et al., 2004). Whether this notion could extend to a possible interplay between the $Ca^{2+}$ entry via NCX and activity of ryanodine/caffeine-sensitive receptors of the ER is not clear due to lack of evidence for spatial association of these proteins; additionally, the role of ryanodine receptors in astrocytic $Ca^{2+}$ excitability remains debatable (Parpura et al., 2011).

Unlike previous studies demonstrating that inhibition of NKA increased basal $[Ca^{2+}]_{cyt}$ in cortical and in cerebellar type 1 astrocytes (Rojas et al., 2004), our treatment with ouabain significantly reduced the basal $[Ca^{2+}]_{cyt}$ in cortical astrocytes (Figure 1A). This observation cannot be explained by an inadequate inhibition of the NKA since in parallel experiments ouabain significantly increased $Na^{+}{}_{cyt}$ accumulation (Figure 1B). The likely explanation for these seemingly disparate findings might be lower temperature in our experiments. Namely, while we recorded at room temperature (22–25°C), above mentioned studies have done so at higher temperatures [32–34°C (Goldman et al., 1994) or 35–37°C

(Rojas et al., 2004)]. If we compare calculated $E_{NCX}$ using our ionic conditions at 25°C (−98 mV) compared with 37°C (−123 mV), we find $E_{NCX}$ to be shifted towards less hyperpolarizing values at room temperature, which would lessen the operation of NCX in the reverse mode. Indeed, it has been reported that NCX activity is greatly inhibited in cultured Purkinje neurons at room temperature (Rojas et al., 2003). Thus, it is possible that reduction in $Ca^{2+}_{cyt}$ during NKA blockade points to restrained operation of NCX in the reverse mode at room temperature, while PMCA activity would remain grossly uninterrupted, as one could expect from difference in turnover rates between the pump and the transporter; PMCA turnover rate is 30–250/s, while that of NCX is 2000–5000/s (Blaustein and Lederer, 1999). In addition, NCX activity requires $Ca^{2+}_{cyt}$ to bind internal regulatory sites, which at the low $[Ca^{2+}]_{cyt}$ and relatively low temperature conditions we tested, may not be optimally engaged (Blaustein and Lederer, 1999). Indeed, when $Ca^{2+}_{cyt}$ was increased by addition of caloxin 2A1, which inhibited the PMCA along with the NKA blockade, the $[Na^+]_{cyt}$ was greatly reduced revealing the operation of NCX in the reverse mode to extrude $Na^+_{cyt}$ while facilitating $Ca^{2+}$ entry (Figure 1). Furthermore, a decrease in basal $[Ca^{2+}]_{cyt}$ due to ouabain treatment and via NCX modulation was occluded when astrocytes were co-treated by benzamil (Figure 1A).

At elevated $[Ca^{2+}]_{cyt}$ induced by mechanical stimulation, the NKA indirectly affected $Ca^{2+}$ homoeostasis as well. Inhibition of NKA decreased the peak but increased cumulative $Ca^{2+}$ accumulation in response to mechanical stimulation (Figure 3). The reduced $Ca^{2+}_{cyt}$ peak response suggests that elevated $Na^+_{cyt}$ initially reduces the activity of the NCX (Blaustein and Lederer, 1999). However, as the NCX activity ramped up, the elimination of the NKA activity as the primary reducer of $Na^+_{cyt}$ significantly increased the cumulative accumulation of $Ca^{2+}_{cyt}$ (Figure 3C). This observation suggests that $Na^+$ extrusion at elevated mechanically induced $Na^+_{cyt}$ is in part mediated by the NCX in exchange for $Ca^{2+}$ entry. It is possible that $Na^+$ extrusion is also mediated by other $Na^+$ extrusion systems, such as the NCKX ($K^+$-dependent NCX) (Kim et al., 2005; Visser and Lytton, 2007), although neurons, but not astrocytes seem to preferentially express NCKX (Kiedrowski et al., 2002). Hence, treatment with ouabain alone or in combination with benzamil did not cause increase in peak and cumulative $Na^+_{cyt}$ accumulation in mechanically stimulated astrocytes, but rather a significant decrease reaching levels similar to that seen in the stimulated astrocytes pre-treated with benzamil alone (Figure 4). This contradicts our previous consideration that decrease in $[Na^+]_{cyt}$ seen in stimulated astrocytes pretreated with benzamil could be due to the NKA activity and might imply an involvement of NCKX in this process. Consequently, although a minor contribution of NCKX is expected (Kiedrowski et al., 2002), its possible role in the regulation of the $Na^+_{cyt}$ and $Ca^{2+}_{cyt}$ in astrocytes needs to be evaluated as it has been done in the calyx of Held (Kim et al., 2005).

The complex interplay between $Na^+_{cyt}$ and $Ca^{2+}_{cyt}$ dynamics and signalling in astrocytes warrants some further considerations. The NKA (type $\alpha 2$) have been found to colocalize with NCX in cortical astrocytes at plasma membrane–ER junctions where tightly regulated 'sodium microdomains' may occur (Juhaszova and Blaustein, 1997; Blaustein et al., 2002). Inhibition of NKA has been shown to generate $Ca^{2+}$ oscillations in cultured hippocampal astrocytes (Liu et al., 2007). In addition, subsets of mitochondria have been shown to interact with the ER (Rizzuto et al., 1998; Csordas et al., 2006). At higher $[Na^+]_{cyt}$ near mitochondria–ER junctions, the driving force for $Ca^{2+}$ efflux from mitochondria via the mitochondrial NCX would increase. Hypothetically, this $Ca^{2+}$ efflux could in turn increase $[Ca^{2+}]_{cyt}$ to activate ryanodine receptor of the ER. Indeed, it appears that the mitochondrial NCX plays a role in $Ca^{2+}_{cyt}$ oscillations (Hernandez-SanMiguel et al., 2006).

Previous work showed that mild depolarization of cortical astrocytes cultured from adult, but not neonatal, rats caused NCX to operate in the reverse mode leading to $[Ca^{2+}]_{cyt}$ increases and consequential exocytotic glutamate release (Paluzzi et al., 2007). Our data are consistent with this finding, yet they add an additional possibility: the involvement of the reverse mode of NCX in mechanically induced glutamate release from neonatal astrocytes. Mechanical stimulation drives $Ca^{2+}$-dependent regulated exocytosis in astrocytes (Hua et al., 2004). The contribution of the NCX in these processes was seen as reduced peak and cumulative $Ca^{2+}_{cyt}$ accumulations (Figures 5A–5C), as well as reduction in peak and cumulative release of glutamate from astrocytes to the ECS (Figures 5G–5I). It should be noted that, consistent with our calculated $E_{NCX}$ at rest and during mechanical stimulation, KB-R7943 blockade of $Ca^{2+}$ entry via the reverse mode of NCX upon mechanical stimulation appeared smaller (85 and 90% of peak and cumulative response of control, respectively) than its effect on reduction of $Ca^{2+}$ entry in astrocytes at rest (72% of basal level) (compare Figure 5A and Figure 1A). Additionally, KB-R7943 significantly reduced peak and cumulative $Na^+_{cyt}$ accumulations (Figures 5D–5F), an indirect effect, likely due to an increased NKA activity, which is in agreement with data obtained using this blocker on astrocytes at rest.

The cellular location of the NCX favours its role in the modulation of $Ca^{2+}$-dependent glutamate release. NCXs are located on plasma membrane–ER junctions and are expressed near $InsP_3$ receptor-gated channels (Lencesova et al., 2004) and NKA (Juhaszova and Blaustein, 1997). Additionally, NCX is co-localized with plasma membrane glutamate transporters in perisynaptic processes (Minelli et al., 2007). Thus, in terms of glutamatergic synaptic transmission, as glutamate is released from neurons, it acts upon the plasma membrane glutamate transporters and ionotropic receptors on astrocytes, which leads to an increase in astrocytic $[Na^+]_{cyt}$ (Langer and Rose, 2009; Lalo et al., 2011). Such $Na^+_{cyt}$ dynamics should lead to depolarization causing NCX to operate in reverse and allow $Ca^{2+}$ entry from the ECS

subsequently stimulating glutamatergic gliotransmission. However, the role of plasma membrane glutamate ionotropic receptors and transporters in exocytotic glutamate release from astrocytes is speculative at the moment. Exposure of cultured cortical astrocytes to AMPA (α-amino-3-hydroxy-5-methylisoxazole-4-propionic acid) did not induce glutamate release, unless it was co-applied with an mGluR agonist (Bezzi et al., 1998); co-application had much greater effect than that of an mGluR agonist alone. While this finding is consistent with the expression of GluR2 subunit in astrocytes, leading to low $Ca^{2+}$ permeability through their AMPA channels, it is at odds with findings that depolarization due to increases in $Na^{+}_{cyt}$ following activation of kainate receptors was reported to stimulate $Ca^{2+}$ entry through the reverse mode of the NCX in specialized astrocytes, the Bergmann glia, in acute slice (Kirischuk et al 1997). These ostensibly incongruent findings could perhaps be due to different spatial associations between NCX, glutamate receptor and secretory machinery in different regions of the brain (cortex against cerebellum), choice of the agonist (AMPA against kainate) and preparation (culture against acute slice). Nonetheless, when operable, this NCX-linked pathway should be faster and spatially more confined, than the parallel pathway engaging astrocytic mGluRs tapping mainly into recruitment of $Ca^{2+}$ from the ER store to cause glutamatergic gliotransmission. Of course, this possibility would need to be corroborated morphologically by studying the spatial relationship between exocytotic proteins, NCX, glutamate receptors and transporters, as well as using electrophysiological recordings from neurons while specifically manipulating NCX in nearby astrocytes.

## ACKNOWLEDGEMENTS

We dedicate this paper to the late Professor Dale J. Benos. We thank Manoj K. Gottipati for comments on a previous version of this paper.

## FUNDING

This work was supported by the National Institute of Mental Health [grant number MH 069791] and the National Science Foundation [grant number CBET 0943343].

## REFERENCES

Araque A, Sanzgiri RP, Parpura V, Haydon PG (1999a) Astrocyte-induced modulation of synaptic transmission. Can. J. Physiol. Pharmacol. 77:699–706.

Araque A, Sanzgiri RP, Parpura V, Haydon PG (1999b) Calcium elevation in astrocytes causes an NMDA receptor-dependent increase in the frequency of miniature synaptic currents in cultured hippocampal neurons. J. Neurosci. 18:6822–6829.

Araque A, Parpura V, Sanzgiri RP, Haydon PG (1999c) Tripartite synapses: glia, the unacknowledged partner. Trends Neurosci. 22:208–215.

Benz B, Grima G, Do KQ (2004) Glutamate-induced homocysteic acid release from astrocytes: possible implication in glia-neuron signaling. Neuroscience 124:377–386.

Bezzi P, Carmignoto G, Pasti L, Vesce S, Rossi D, Rizzini BL, Pozzan T, Volterra A (1998) Prostaglandins stimulate calcium-dependent glutamate release in astrocytes. Nature 391:281–285.

Blaustein MP, Lederer WJ (1999) Sodium/calcium exchange: its physiological implications. Physiol. Rev. 79:763–854.

Blaustein MP, Juhaszova M, Golovina VA, Church PJ, Stanley EF (2002) Na/Ca exchanger and PMCA localization in neurons and astrocytes: functional implications. Ann. NY Acad. Sci. 976:356–366.

Chaudhary J, Walia M, Matharu J, Escher E, Grover AK (2001) Caloxin: a novel plasma membrane $Ca^{2+}$ pump inhibitor. Am. J. Physiol. Cell Physiol. 280:C1027–1030.

Clapham DE (2003) TRP channels as cellular sensors. Nature 426:517–524.

Csordas G, Renken C, Varnai P, Walter L, Weaver D, Buttle KF, Balla T, Mannella CA, Hajnoczky G (2006) Structural and functional features and significance of the physical linkage between ER and mitochondria. J. Cell. Biol. 174:915–921.

De Luisi A, Hofer AM (2003) Evidence that $Ca^{(2+)}$ cycling by the plasma membrane $Ca^{(2+)}$-ATPase increases the 'excitability' of the extracellular $Ca^{(2+)}$-sensing receptor. J. Cell. Sci. 116:1527–1538.

Deitmer JW (2004) pH regulation and acid/base-mediated transport in glial cells. In: Glial-Neuronal Signaling (Hatton GI, Parpura V, eds.), pp. 263–277. Boston, MA: Kluwer Academic Publishers.

DiPolo R, Beauge L (1979) Physiological role of ATP-driven calcium pump in squid axon. Nature 278:271–273.

Filosa JA, Bonev AD, Nelson MT (2004) Calcium dynamics in cortical astrocytes and arterioles during neurovascular coupling. Circ. Res. 95:e73–81.

Fresu L, Dehpour A, Genazzani AA, Carafoli E, Guerini D (1999) Plasma membrane calcium ATPase isoforms in astrocytes. Glia 28:150–155.

Goldman WF, Yarowsky PJ, Juhaszova M, Krueger BK, Blaustein MP (1994) Sodium/calcium exchange in rat cortical astrocytes. J. Neurosci. 14:5834–5843.

Gordon GR, Mulligan SJ, MacVicar BA (2007) Astrocyte control of the cerebrovasculature. Glia 55:1214–1221.

Haydon PG, Carmignoto G (2006) Astrocyte control of synaptic transmission and neurovascular coupling. Physiol. Rev. 86:1009–1031.

He S, Ruknudin A, Bambrick LL, Lederer WJ, Schulze DH (1998) Isoform-specific regulation of the $Na^{+}/Ca^{2+}$ exchanger in rat astrocytes and neurons by PKA. J. Neurosci. 18:4833–4841.

Hernandez-SanMiguel E, Vay L, Santo-Domingo J, Lobaton CD, Moreno A, Montero M, Alvarez J (2006) The mitochondrial $Na^{+}/Ca^{2+}$ exchanger plays a key role in the control of cytosolic $Ca^{2+}$ oscillations. Cell Calcium 40:53–61.

Hua X, Malarkey EB, Sunjara V, Rosenwald SE, Li WH, Parpura V (2004) $Ca^{2+}$-dependent glutamate release involves two classes of endoplasmic reticulum $Ca^{2+}$ stores in astrocytes. J. Neurosci. Res. 76:86–97.

Innocenti B, Parpura V, Haydon PG (2000) Imaging extracellular waves of glutamate during calcium signaling in cultured astrocytes. J. Neurosci. 20:1800–1808.

Juhaszova M, Blaustein MP (1997) Na+ pump low and high ouabain affinity alpha subunit isoforms are differently distributed in cells. Proc. Natl. Acad. Sci. U.S.A. 94:1800–1805.

Kawano S, Otsu K, Shoji S, Yamagata K, Hiraoka M (2003) $Ca^{(2+)}$ oscillations regulated by $Na^{(+)}$-$Ca^{(2+)}$ exchanger and plasma membrane $Ca^{(2+)}$ pump induce fluctuations of membrane currents and potentials in human mesenchymal stem cells. Cell Calcium 34:145–156.

Kiedrowski L, Czyz A, Li XF, Lytton J (2002) Preferential expression of plasmalemmal K-dependent $Na^{+}/Ca^{2+}$ exchangers in neurons versus astrocytes. Neuroreport 13:1529–1532.

Kim MH, Korogod N, Schneggenburger R, Ho WK, Lee SH (2005) Interplay between Na+/Ca2+ exchangers and mitochondria in $Ca^{2+}$ clearance at the calyx of Held. J. Neurosci. 25:6057–6065.

Kirischuk S, Kettenmann H, Verkhratsky A (1997) $Na^{+}/Ca^{2+}$ exchanger modulates kainate-triggered $Ca^{2+}$ signaling in Bergmann glial cells *in situ*. FASEB J. 11:566–572.

Kirischuk S, Kettenmann H, Verkhratsky A (2007) Membrane currents and cytoplasmic sodium transients generated by glutamate transport in Bergmann glial cells. Pflugers Arch. 454:245–252.

Kucheryavykh YV, Kucheryavykh LY, Nichols CG, Maldonado HM, Baksi K, Reichenbach A, Skatchkov SN, Eaton MJ (2007) Downregulation of Kir4.1 inward rectifying potassium channel subunits by RNAi impairs potassium transfer and glutamate uptake by cultured cortical astrocytes. Glia 55:274–281.

Lalo U, Pankratov Y, Parpura V, Verkhratsky A (2011) Ionotropic receptors in neuronal-astroglial signalling: what is the role of 'excitable' molecules in non-excitable cells. Biochim. Biophys. Acta 1813:992–1002.

Lalo U, Pankratov Y, Kirchhoff F, North RA, Verkhratsky A (2006) NMDA receptors mediate neuron-to-glia signaling in mouse cortical astrocytes. J. Neurosci. 26:2673–2683.

Lalo U, Pankratov Y, Wichert SP, Rossner MJ, North RA, Kirchhoff F, Verkhratsky A (2008) P2 × 1 and P2 × 5 subunits form the functional P2X receptor in mouse cortical astrocytes. J. Neurosci. 28:5473–5480.

Langer J, Rose CR (2009) Synaptically induced sodium signals in hippocampal astrocytes *in situ*. J. Physiol. 587:5859–5877.

Lee W, Malarkey EB, Reyes RC, Parpura V (2008) Micropit: a new cell culturing approach for characterization of solitary astrocytes and small networks of these Glial cells. Front Neuroeng. 1:2.

Lencesova L, O'Neill A, Resneck WG, Bloch RJ, Blaustein MP (2004) Plasma membrane–cytoskeleton–endoplasmic reticulum complexes in neurons and astrocytes. J. Biol. Chem. 279:2885–2893.

Liu XL, Miyakawa A, Aperia A, Krieger P (2007) Na,K-ATPase generates calcium oscillations in hippocampal astrocytes. Neuroreport 18:597–600.

Magistretti PJ (2006) Neuron-glia metabolic coupling and plasticity. J. Exp. Biol. 209:2304–2311.

Malarkey EB, Parpura V (2011) Temporal characteristics of vesicular fusion in astrocytes: examination of synaptobrevin 2-laden vesicles at single vesicle resolution. J. Physiol. 589:4271–4300.

Malarkey EB, Ni Y, Parpura V (2008) $Ca^{2+}$ entry through TRPC1 channels contributes to intracellular $Ca^{2+}$ dynamics and consequent glutamate release from rat astrocytes. Glia 56:821–835.

Maroto R, Raso A, Wood TG, Kurosky A, Martinac B, Hamill OP (2005) TRPC1 forms the stretch-activated cation channel in vertebrate cells. Nat. Cell Biol. 7:179–185.

Mata M, Fink DJ (1989) $Ca^{++}$-ATPase in the central nervous system: an EM cytochemical study. J. Histochem. Cytochem. 37:971–980.

McCarthy KD, de Vellis J (1980) Preparation of separate astroglial and oligodendroglial cell cultures from rat cerebral tissue. J. Cell. Biol. 85:890–902.

Meier SD, Kovalchuk Y, Rose CR (2006) Properties of the new fluorescent Na+ indicator CoroNa Green: comparison with SBFI and confocal $Na^+$ imaging. J. Neurosci. Methods 155:251–259.

Minelli A, Castaldo P, Gobbi P, Salucci S, Magi S, Amoroso S (2007) Cellular and subcellular localization of $Na^+$–$Ca^{2+}$ exchanger protein isoforms, NCX1, NCX2, and NCX3 in cerebral cortex and hippocampus of adult rat. Cell Calcium 41:221–234.

Montana V, Ni Y, Sunjara V, Hua X, Parpura V (2004) Vesicular glutamate transporter-dependent glutamate release from astrocytes. J. Neurosci. 24:2633–2642.

Morgans CW, El Far O, Berntson A, Wassle H, Taylor WR (1998) Calcium extrusion from mammalian photoreceptor terminals. J. Neurosci. 18:2467–2474.

Mothet JP, Pollegioni L, Ouanounou G, Martineau M, Fossier P, Baux G (2005) Glutamate receptor activation triggers a calcium-dependent and SNARE protein-dependent release of the gliotransmitter D-serine. Proc. Natl. Acad. Sci. U.S.A. 102:5606–5611.

Mulligan SJ, MacVicar BA (2004) Calcium transients in astrocyte endfeet cause cerebrovascular constrictions. Nature 431:195–199.

Ni Y, Malarkey EB, Parpura V (2007) Vesicular release of glutamate mediates bidirectional signaling between astrocytes and neurons. J. Neurochem. 103:1273–1284.

Paluzzi S, Alloisio S, Zappettini S, Milanese M, Raiteri L, Nobile M, Bonanno G (2007) Adult astroglia is competent for $Na^+/Ca^{2+}$ exchanger-operated exocytotic glutamate release triggered by mild depolarization. J. Neurochem. 103:1196–1207.

Parpura V, Haydon PG (2000) Physiological astrocytic calcium levels stimulate glutamate release to modulate adjacent neurons. Proc. Natl. Acad. Sci. U.S.A. 97:8629–8634.

Parpura V, Zorec R (2010) Gliotransmission: exocytotic release from astrocytes. Brain Res. Rev. 63:83–92.

Parpura V, Grubisic V, Verkhratsky A (2011) $Ca^{2+}$ sources for the exocytotic release of glutamate from astrocytes. Biochim. Biophys. Acta 1813:984–991.

Parpura V, Fang Y, Basarsky T, Jahn R, Haydon PG (1995) Expression of synaptobrevin II, cellubrevin and syntaxin but not SNAP-25 in cultured astrocytes. FEBS Lett. 377:489–492.

Perea G, Araque A (2007) Astrocytes potentiate transmitter release at single hippocampal synapses. Science 317:1083–1086.

Perea G, Araque A (2009) Synaptic information processing by astrocytes. In: Astrocytes in (patho)physiology of the Nervous System (Parpura V, Haydon PG, eds.), pp. 287–300. New York, NY: Springer.

Perea G, Navarrete M, Araque A (2009) Tripartite synapses: astrocytes process and control synaptic information. Trends Neurosci. 32:421–431.

Regehr WG (1997) Interplay between sodium and calcium dynamics in granule cell presynaptic terminals. Biophys. J. 73:2476–2488.

Reyes RC, Parpura V (2008) Mitochondria modulate Ca2+-dependent glutamate release from rat cortical astrocytes. J. Neurosci. 28:9682–9691.

Reyes RC, Parpura V (2009) Modulation of $Ca^{2+}$-dependent glutamate release in rat cortical astrocytes by the $Na^+/Ca^{2+}$ exchanger. J. Neurochem. 108:116–117.

Reyes RC, Perry G, Lesort M, Parpura V (2011) Immunophilin deficiency augments Ca2+-dependent glutamate release from mouse cortical astrocytes. Cell Calcium 49:23–34.

Rizzuto R, Pinton P, Carrington W, Fay FS, Fogarty KE, Lifshitz LM, Tuft RA, Pozzan T (1998) Close contacts with the endoplasmic reticulum as determinants of mitochondrial Ca2+ responses. Science 280:1763–1766.

Rojas H, Ramos M, Dipolo R (2004) A genistein-sensitive Na+/$Ca^{2+}$ exchange is responsible for the resting $[Ca^{2+}]i$ and most of the $Ca^{2+}$ plasma membrane fluxes in stimulated rat cerebellar type 1 astrocytes. Japan. J. Physiol. 54:249–262.

Rojas H, Ramos M, Mijares A, DiPolo R (2003) Role of $Na^+/Ca^{2+}$ exchange in $[Ca^{2+}]$i clearance in rat culture Purkinje neurons requires reevaluation. Japan. J. Physiol. 53:259–269.

Rojas H, Colina C, Ramos M, Benaim G, Jaffe EH, Caputo C, DiPolo R (2007) $Na^+$ entry via glutamate transporter activates the reverse Na+/$Ca^{2+}$ exchange and triggers Ca(i)2+-induced $Ca^{2+}$ release in rat cerebellar Type-1 astrocytes. J. Neurochem. 100:1188–1202.

Rose CR, Ransom BR (1997) Gap junctions equalize intracellular $Na^+$ concentration in astrocytes. Glia 20:299–307.

Rychkov G, Barritt GJ (2007) TRPC1 Ca(2+)-permeable channels in animal cells. Handb. Exp. Pharmacol. 179:23–52.

Suzuki A, Stern SA, Bozdagi O, Huntley GW, Walker RH, Magistretti PJ, Alberini CM (2011) Astrocyte-neuron lactate transport is required for long-term memory formation. Cell 144:810–823.

Theodosis DT, Poulain DA, Oliet SH (2008) Activity-dependent structural and functional plasticity of astrocyte-neuron interactions. Physiol. Rev. 88:983–1008.

Verkhratsky A, Orkand RK, Kettenmann H (1998) Glial calcium: homeostasis and signaling function. Physiol. Rev. 78:99–141.

Visser F, Lytton J (2007) K+ -dependent $Na^+/Ca^{2+}$ exchangers: key contributors to $Ca^{2+}$ signaling. Physiology (Bethesda) 22:185–192.

Zhong N, Beaumont V, Zucker RS (2001) Roles for mitochondrial and reverse mode $Na^+/Ca^{2+}$ exchange and the plasmalemma $Ca^{2+}$ ATPase in post-tetanic potentiation at crayfish neuromuscular junctions. J. Neurosci. 21:9598–9607.

Zonta M, Angulo MC, Gobbo S, Rosengarten B, Hossmann KA, Pozzan T, Carmignoto G (2003) Neuron-to-astrocyte signalling is central to the dynamic control of brain microcirculation. Nat. Neurosci. 6:43–50.

**Received 5 December 2011/18 January 2012; accepted 20 January 2012**

**Published as Immediate Publication 23 January 2012, doi 10.1042/AN20110059**